J Mater Sci (2011) 46:7377–7383
DOI 10.1007/s10853-011-5698-y

An experimental refinement of solid–solution relationship in Ca-α-Sialon ceramics by analytical electron microscopy

Bo Zhu · Hui Gu · Pei-ling Wang

Received: 21 February 2011 / Accepted: 6 June 2011 / Published online: 25 June 2011

Abstract Local dopant compositions within individual α-Sialon grains were measured by analytical electron microscopy (AEM) in hot-pressed $Ca_xSi_{12-3x}Al_{3x}O_xN_{16-x}$ ($x = 0.3$–1.4) ceramics. The reduction of local x values from the nominal dopant compositions is about 40% in general, and it reaches 60% for the end member ($x = 1.4$) which contains inclusions of AlN-based 21R phase. This results exhibit stronger departures from x than the previous report of 30% dopants missing in α-Sialon phase by electron probe micro-analysis (EPMA) [J Eur Ceram Soc 19:1637, 1999]. Amorphous films of ~1 nm thick were commonly found at grain boundaries (GBs), which could only take a small fraction of undetected dopants while the film composition exhibits a quite different behavior. The general presence of GB films can rationalize the discrepancy between AEM and EPMA results by their differences in probe size and detection geometry, while the much larger gap in the end member suggests the existence of Ca-rich glasses in the intergranular regions. By excluding this end member, a linear relation between dopant solution and lattice expansion is restored in α-Sialon structure, which leads to 20 and 80% increases of the expansion coefficients from those given in the previous and original reports, respectively. This study not only demonstrated the necessity of solubility study in ceramics by AEM refinement, but also opens a new front to correlate the solution behavior with the intergranular glass/amorphous structures, both were regarded so far as largely independent.

B. Zhu · H. Gu (✉) · P. Wang
State Key Laboratory of High Performance Ceramics and Superfine Microstructures, Shanghai Institute of Ceramics, Chinese Academy of Sciences, Shanghai 200050, China
e-mail: gu@mail.sic.ac.cn

Present Address:
B. Zhu
Jinma Corp, Dalian, China

Introduction

The α-Sialon material is an important structure ceramic with excellent hardness and strength, especially retaining large strength at high temperatures [1–3]. As a solid solution of α-Si_3N_4, it has a general formula as $M_xSi_{12-(m+n)}Al_{m+n}O_nN_{16-n}$ ($x = m/v \leq 2$, and v is the valance of metal filled into the empty cages in lattice) where the metal filler serves for charge balance and it could be Li, Mg, Ca, Sc, Y, or rare-earths (REs). The key advantage of α-Sialon phase lies in its capacity to absorb most sintering aides (mainly metal oxides) into the lattice to minimize the presence of residual phases at intergranular regions, hence leading to improved high temperature performance [2, 4, 5]. In recent years, most studies on α-Sialon have focused on Y- and RE-α-Sialon due to their capacity in microstructure tailoring as well as the reversible phase transitions, but these dopants were found unstable in the α-Sialon phase especially for light RE elements, hence restricting their applications at high temperature [5–8]. On the other hand, Ca-α-Sialon has a rather wide range of solid–solution to facilitate a more effective cleaning of the residual liquid from grain boundary (GB), while it has exhibited also a better thermal stability to suppress the phase evolution at high temperature [2, 9]. Both characters enable the Ca-α-Sialon being an ideal system to revealing representative characteristics or behaviors for dopant solution in ceramics before considering extrinsic or microstructure factors [4, 10].

The dopant–solution relationship in ceramics is conventionally studied by powder X-ray diffraction (XRD) that takes all the dopants as the solutes, similar to other materials systems [4]. Electron probe microanalysis (EPMA) is often used to validate or improve such a global dopant-solute correlation based on measurements at a micrometer scale. In recent years, however, our experimental studies at a nanometer scale by analytical electron microscopy (AEM) methods indicate that the solid–solution characteristics in ceramic materials exhibited often a different pattern from the global dopants, such as in the cases of TiO_2-doped Al_2O_3, CeO_2-doped ZrO_2, and AlN-doped SiC [11–14]. The ~1 nm thick amorphous films at GB often accommodate disproportional amounts of dopants, especially when the grain sizes are smaller than 1 μm [15–17]. Similar situation should not elude α-Sialon ceramics: indeed we have observed a different solid–solution relation in RE-α-Sialon system from the nominal dopant trend by applying this unconventional method [5]. In this article, we will report an AEM study to measure the local solid–solution relationship in Ca-α-Sialon in comparison with the previously reported EPMA study [4, 10]. This may gain a refined picture of dopant–solute correlation in this ceramic system, which could serve as a model or starting case for similar and future studies.

Experimental

Ca-α-Sialon materials were hot-pressed under 20 MPa at 1750 °C for 1 h in a graphite-resistant furnace in flowing nitrogen of 1 atm. The starting powders were a mixture of Si_3N_4 (E-10, Ube, Japan) with 2 wt% O, AlN with 1.3 wt% O, and $CaCO_3$ of 99.0% purity following the formula of $Ca_xSi_{12-3x}Al_{3x}O_{16-x}$ with $x = 0.3$, 0.6, 1.0, 1.4, respectively, which takes $m = 2n$ in the general formula, or $x = n = m/2$. Each mixture was kept at 1150 °C for 0.5 h to complete the decomposition of $CaCO_3$ before sintering. The resultant ceramics are hereafter abbreviated as CA03, CA06, CA10, and CA14. More details of the materials processing can be found in Ref. [4], which has also presented a joint XRD and EPMA analysis of dopant solution characteristics for these samples, except for CA30 due to the presence of β-Sialon phase [10].

Thin foils for transmission electron microscopy (TEM) investigation were prepared by standard routine of cutting, grinding, dimpling, and finally argon-ion-milling to reach transparency for electron. Carbon coating is applied to reduce charging during TEM observations. TEM/AEM investigation was performed with an electron microscope operated at 200 kV (Model 2010, JEOL, Tokyo, Japan) equipped with an X-ray spectrometer (Link/ISIS, Oxford Instrument, England) for EDXS (energy-dispersive X-ray spectroscopy) analysis.

Quantitative compositional analysis by EDXS in TEM constitutes the main part of this AEM study, which employs an electron probe of 20–30 nm. Since the anions N and O are not sensitive to EDXS quantification hence less reliable, we focus on the cations Al and Ca to measure the solution levels in Si-based grains, based on the Cliff–Lorimer relation [18]. The *k*-factors involved in the cation quantification are obtained from the standard-less routine with a ZAF correction. The contribution of surface effect resulted from ion-milling was found insignificant, as evaluated following an approach described in [11]. The segregation of dopants to GB was measured by the spatially resolved EDXS method by placing the electron probe at GB and the nearby grains, respectively, to yield an excess at GB, following Refs. [15, 16]:[1]

$$\Gamma_i = \left(C_i^{\mathrm{GB}} - C_i^{\mathrm{b}}\right) \cdot N_{\mathrm{r}}^{\mathrm{b}} \cdot \left(\frac{\pi \cdot D}{4}\right) \quad (1)$$

where C_i is concentration and the superscripts "GB" and "b" (for "bulk") denote the respective positions. $N_{\mathrm{r}}^{\mathrm{b}}$ is the atomic site density of the reference element (Si) in the bulk, which is calculated from the actual Si content in individual α-Sialon grains. D is the probe diameter and $\pi/4$ is a geometric factor to count for the round shaped beam. The probe size was measured directly from the imaging screen as 23 ± 2 nm.

Result and discussions

The microstructure of Ca-α-Sialon ceramics typically consists of equiaxed grains of size between 0.5 and 1 μm as shown in Fig. 1a. CA03 is the only sample containing elongated β-Sialon grains, which is not as dense as other samples, most likely due to the lack of enough liquid during sintering. In addition, Al-rich inclusions were often found in CA14 (Fig. 1b), and they should correspond to the weak presence of 21R-polytypoid oxynitride phase $SiAl_6O_2N_6$ as detected by XRD in this sample, as confirmed by EDXS measurements to reveal the AlN-based composition (Fig. 1c). In addition, there has been also a trace level of 21R phase detected in CA10. These minor phases are listed in Table 1.

Solute levels for Ca and Al measured from individual α-Sialon grains are all given in Fig. 2. Each datum takes an average of 2–3 measurements to ensure the repeatability, hence the improved reliability. The Al and Ca solution in each sample are relatively uniform from grain to grain,

[1] This formula of excess evaluation was mistakenly presented in Ref. [5] where the wrong $(\pi/4)^{1/2}$ was used instead of the correct geometric factor $(\pi/4)$, although actual data in that article had followed the correct formula of Eq. 1 in this article.

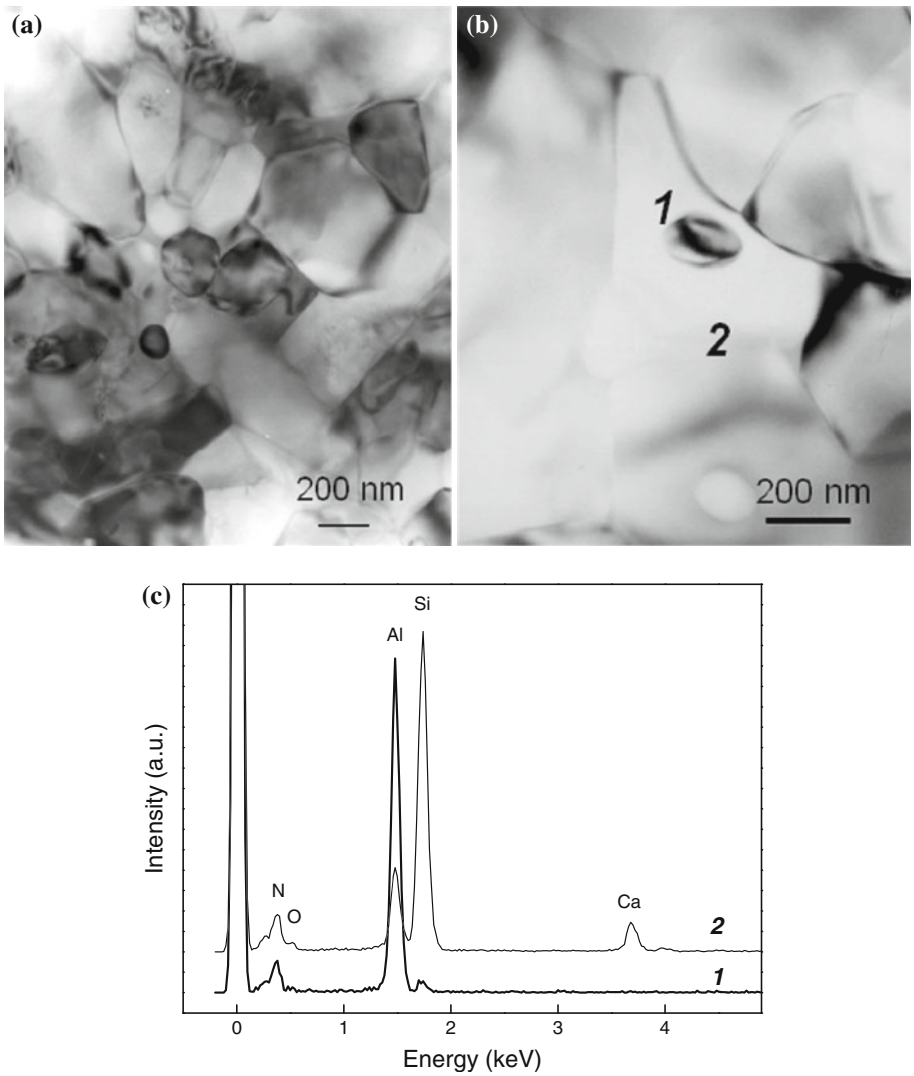

Fig. 1 TEM images of typical microstructures in Ca-α-Sialon: **a** monolithic α-Sialon phase in CA06, **b** 21R inclusions in CA14. EDXS spectra of a 21R inclusion (*1*) and a Sialon grain (*2*) in CA14 are given in **c**

Table 1 Comparison of x values in $Ca_xSi_{12-3x}Al_{3x}O_xN_{16-x}$ determined from different methods

Sample	Nominal x	From EPMA [4]	By AEM	2nd phase
CA03	0.3	–	0.25 ± 0.06	β
CA06	0.6	0.4	0.36 ± 0.06	–
CA10	1.0	0.7	0.64 ± 0.07	21R[a]
CA14	1.4	0.9	0.48 ± 0.05	21R[b]

[a] Trace

[b] Weak

except the few β-Sialon grains in CA03 revealing no Ca and much less Al. The measured solution levels increased steadily with the nominal dopant level, except for CA10 to exhibit a much faster increase in measured solution even to exceed those in CA14 that contains more dopants. The actual x values of α-Sialon phase in these samples are deduced from the Ca and Al solution measured over many grains, which are given in Table 1 together with the nominal and EPMA values.

The dopants were also segregated at GB to form ~1 nm thick amorphous film in every sample, as exemplified in Fig. 3a. However, the segregation behaviors are rather different from sample to sample, especially in CA10 where the Al segregation is quite abnormal since the measured Al level in GB is even lower than its solution level in the adjacent grain (Fig. 3b). To fully compare the opposite trends, all measured Ca and Al excesses from individual GBs in CA06 and CA10 are given together in Fig. 3c; both

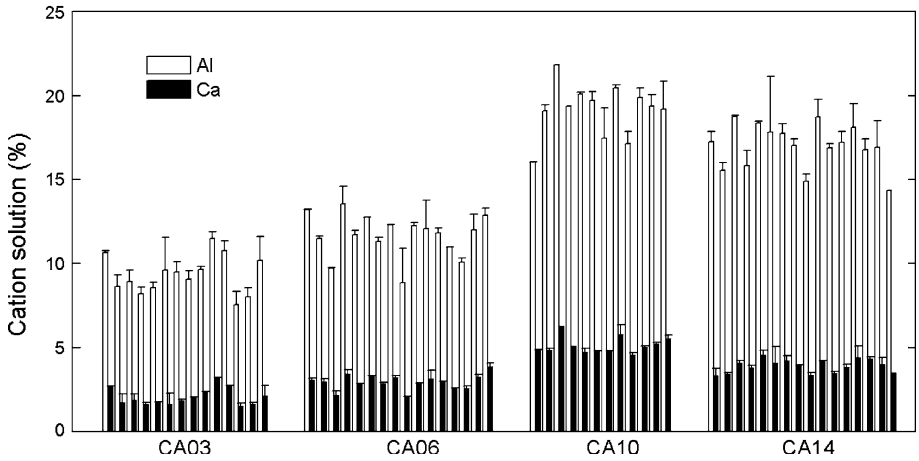

Fig. 2 Distributions of solution levels in individual α-Sialon grains measured by EDXS in this series of Ca-α-Sialon samples

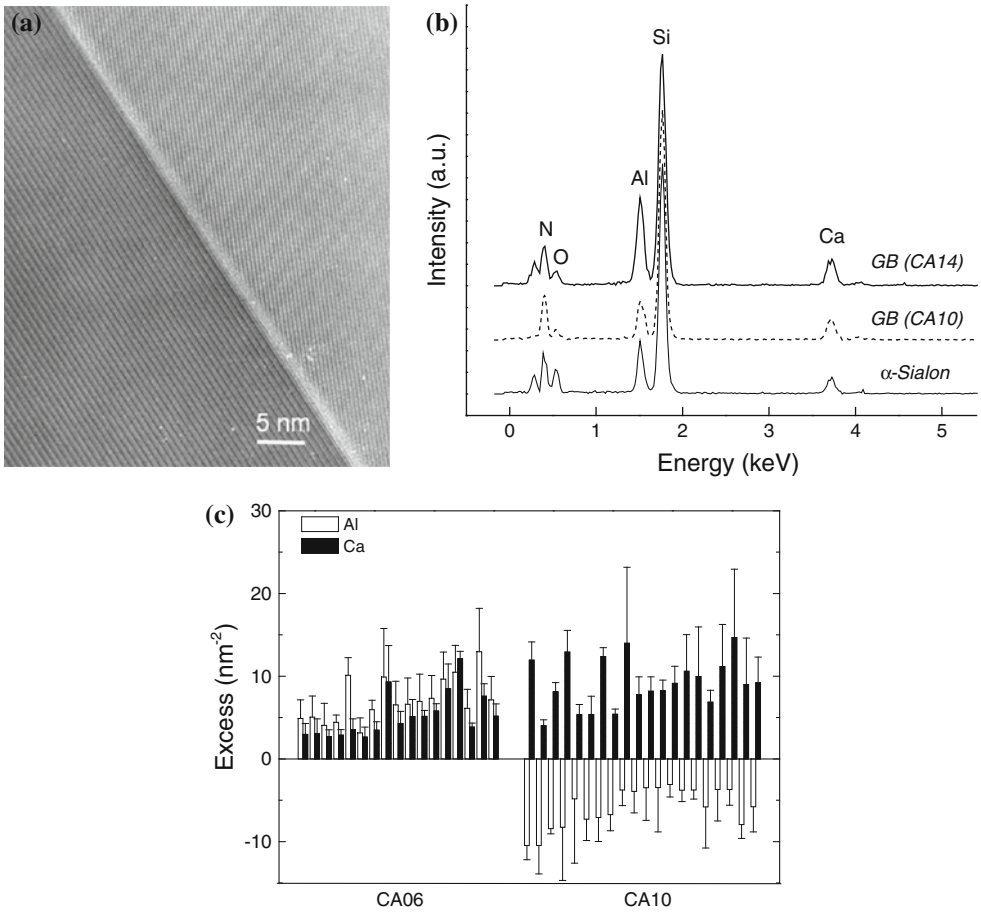

Fig. 3 **a** HRTEM image of an amorphous GB film in Ca-α-Sialon. Typical EDXS spectra (**b**) and all measured excesses (**c**) both reveal that the films compositions are rather different in CA06 and in CA10

samples are almost monolithic α-Sialon materials free from minor phases. The excess level is generally much inaccurate as the solution level since the former cannot be measured directly while dependent on the latter in each measurement [5, 12, 13]. There is a sharp drop in Al dopant accommodated in GB film that turns Al excess in CA06 to Al depletion in CA10, while accompanying a moderate increase, or a normal behavior, in Ca segregation. Such a depletion of Al dopant from GB film can compensate only a small fraction of excessive Al dopant solution in α-Sialon phase observed in CA10, mainly because that thin GB films were largely made of silica [15, 20]. Therefore, GB films play only a minor role in dopant distribution behavior than the solution in α-Sialon phase.

Differences between the measured dopant solutions in Ca-α-Sialon by EPMA and AEM may be due to a

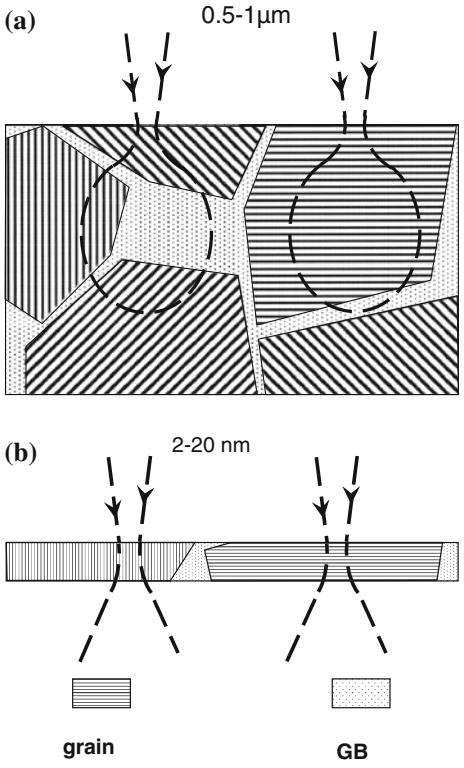

Fig. 4 Schematic diagrams of the analyzed volume probed by electron beam in **a** EPMA and **b** AEM modes

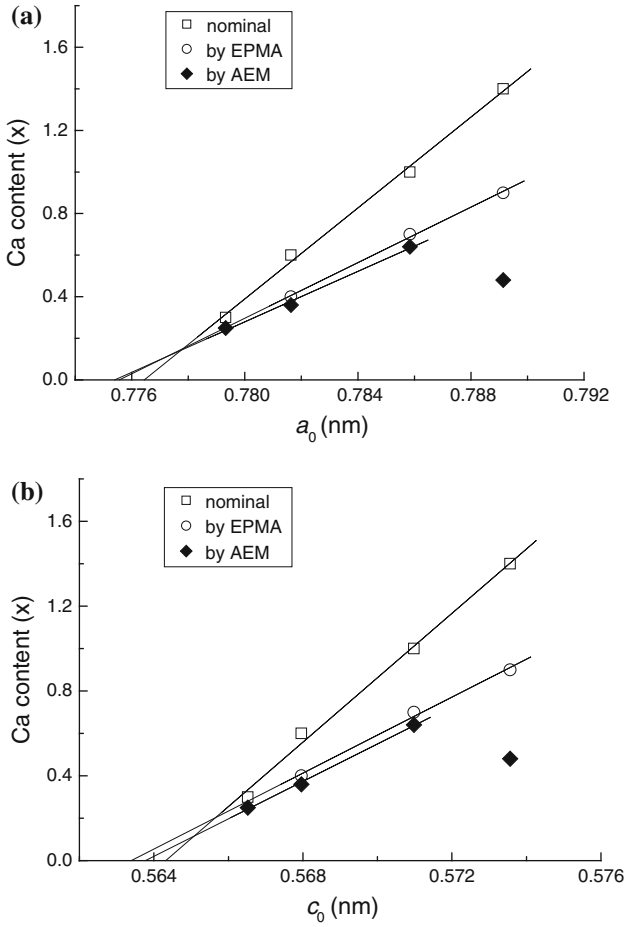

Fig. 5 Unit cell parameters a_0 (**a**) and c_0 (**b**) of α-Sialon phase (measured by XRD, taken from Ref. [4]) versus three sets of x values obtained by three methods. See details in text

combined effect of detection limitation and the presence of intergranular phases. In the CA06 and CA10, the actual x values measured by AEM differ only 10% from the previous results by EPMA [4]. By taking into account of Ca excess at GBs, results from both methods should be even closer to each other. In contrast, the locally measured x in CA14 was below the value in CA10 as measured by AEM, and down to roughly half of the value measured by EPMA (see Fig. 2; Table 1). This discrepancy may be explained by different effects of a Ca-rich intergranular glassy phase possibly presented in this highly doped sample as schematically illustrated in Fig. 4a, b for EPMA and AEM, respectively. The deeply penetrating and much large electron probe (both in the order of ~1 μm) in EPMA analysis of bulk specimens can easily pick up the signal of Ca-rich intergranular glass regions underneath the directly targeted α-Sialon grains, which are generally in sizes of 0.5–1 μm. In contrast, the well-confined AEM probe can hardly extend outside the targeted zone in a grain through thin TEM foils of typically 20–50 nm thick to be suitable for EDXS analysis. The presence of Ca-rich intergranular glasses can explain such a large discrepancy between the two measured Ca solution levels in α-Sialon phase in CA14. Indeed, a similar case of Nd-rich intergranular glass phase had been reported earlier in Nd-α-Sialon [5]. In fact, the EPMA results had found always ~70% of dopants in the α-Sialon phase, which had already interpreted the missing dopants by the presence of intergranular glass phases [4]. Nevertheless, detailed investigation on such possible intergranular structures was not attempted in this study. This is partially because that a recent study of low-CaO-doped Si_3N_4 ceramics had revealed a complex substructure within Ca-rich glassy pockets by an elaborate electron energy-loss spectroscopy analysis of both cations and anions with a sub-nanometer probe [19, 20]. A similar study is beyond the scope of this study, and it may be the subject of future study.

To further reveal the true dopant–solution trend in α-Sialon structure, we plot all three sets of x values versus the lattice parameters a_0 and c_0 of α-Sialon phases as taken from Ref. [4] in Fig. 5a, b, respectively. By excluding the datum for CA14, a linear relation for dopant solution can be similarly deduced with the AEM set as for the EPMA

sets. Three dopant–structure relationships for Ca-α-Sialon structure are thus obtained respectively for nominal dopant level x_N:

$$\Delta a_0 = 0.0091x_N,\ \Delta c_0 = 0.0066x_N, \quad (2)$$

for solution measured by EPMA, or x_E:

$$\Delta a_0 = 0.0149x_E,\ \Delta c_0 = 0.0111x_E, \quad (3)$$

and for solution measured by AEM, or x_A:

$$\Delta a_0 = 0.0164x_A,\ \Delta c_0 = 0.0113x_A \quad (4)$$

with all units in nanometer. The relatively small coefficients in the nominal relation between dopant and structure (Eq. 2) are quite close to the original coefficients reported first by Hampshire et al. [1]:

$$\Delta a_0 = 0.0099x,\ \Delta c_0 = 0.0088x \quad (2')$$

when taking $m = 2n$ (hence $n = x = m/2$). Both cases have under-estimated the effect of dopant on lattice expansion, apparently due to an over-estimation of the solution level by taking all the dopants into α-Sialon phase. On the other hand, the relationship obtained by EPMA (Eq. 3) is very close to those from van Rutten et al. [21] using a same measurement:

$$\Delta a_0 = 0.0137x,\ \Delta c_0 = 0.0105x, \quad (3')$$

both revealing about 70% of dopants as solutes in the lattice with remaining dopants considered to stay in glass phases [4]. The AEM method gave the largest coefficients for lattice expansion (Eq. 4) by detecting even less dopant in the main α-Sialon phase, hence resulting more reliable solubility as well as the refined thermal expansion coefficients.

The new dopant solution trend by AEM indicates not only less solution of dopants into Ca-α-Sialon structure, but the maximum solution level (or solubility) in CA10 has also been reduced significantly from the previous value of about 0.9 down to 0.64, which is rather close to the limit for rare-earth modifiers [6, 9]. In another word, the nominal limit of dopant for single-phased Ca-α-Sialon materials has shifted from $x = 1.4$ down to 1.0, which is due to the joint appearance of large number of Al-rich 21R inclusions and strong increase of Ca-rich intergranular glass phase in the end member CA14. The glass phases had been estimated to take generally 30% of dopants in general by the previous EPMA study [4, 21]; by this study, this effect is further increased to 35–40% of dopants in CA06 and CA10 while jumping to 65% in CA14, a surprising high level. Nevertheless, even the more "reasonable" estimation of 30–40% dopants to stay in intergranular glasses are uncommon, indicating the necessity of a specific and detailed study in future on this abnormal phenomenon, similar to the cases of CaO-doped Si_3N_4 and RE-α-Sialon [5, 19].

Conclusions

(1) Local dopant solution in hot-pressed Ca-α-Sialon ceramics measured by AEM analysis not only confirms the significant less dopants in the α-Sialon phase as reported by earlier EPMA study [4], but also further pushed down the solution level from ~70% by EPMA to ~60% in general by AEM, and even down to ~40% in the high-doping end member with large numbers of 21R inclusions.

(2) Thin amorphous films are common at GB in α-Sialon materials and can take a small fraction of residual dopants, leaving Ca-rich glass phases to accommodate for the remaining dopants. Such GB films and Ca-rich glasses can narrow/remove the discrepancy between AEM and EPMA, due to their difference in analyzed scale and depth. The film composition follows a different behavior as dopant solution, e.g., the depletion of Al at GB in CA10 with the highest solution level.

(3) A new relation between solution and lattice expansion in α-Sialon structure is deduced by excluding the non-single-phased CA14, leading to an increase of 20% in the expansion coefficients over EPMA or an increase of 80% over the nominal dopant solution.

Acknowledgements This study is financially supported by the Natural Science Foundation Committee (Grant No. 50525205). The authors would like to thank Dr. Chen Zhang for materials processing, Ms. Ying-Xin Jia for powder XRD analysis, and Dr. Peng-Xiang Qian for assistance in the preparation of figures.

References

1. Hampshire S, Park HK, Thompson DP, Jack KH (1978) Nature 274:880
2. Hewett CL, Cheng YB, Muddle BC, Trigg MB (1998) J Am Ceram Soc 81:1781
3. Oyama Y, Kamigaito O (1971) Jpn J Appl Phys 10:1637
4. Wang PL, Zhang C, Sun WY, Yan DS (1999) J Eur Ceram Soc 19:553
5. Zhu B, Gu H, Holzer S, Hoffmann MJ (2006) Scr Mater 54:1469
6. Huang ZK, Tien TY, Yan DS (1986) J Am Ceram Soc 69:C241
7. Wang PL, Sun WY, Yen TS (1994) Eur J Solid State Inorg Chem 31:93
8. Mandal H, Camscu N, Thompson DP (1995) J Mater Sci 30:5901. doi:10.1007/BF01151503
9. Huang ZK, Sun WY, Yan DS (1984) J Mater Sci Lett 4:255
10. Wang PL, Jia YX, Zhang C, Sun WY (1999) J Inorg Mater (in Chinese) 14:763
11. Chi MF, Gu H, Wang X, Wang PL (2003) J Am Ceram Soc 86:1953
12. Chi MF, Gu H, Qian PX, Wang X, Wang PL (2005) Int J Mater Res 96:486
13. Fang PA, Gu H, Van Landuyt J, Vleugels J, Vander Biest O, Wang PL (2005) J Am Ceram Soc 88:1929

14. Hu JF, Gu H, Chen ZM, Tan SH, Jiang DL, Rühle M (2007) Acta Mater 55:5666
15. Gu H, Cannon RM, Rühle M (1998) J Mater Res 13:376
16. Chi MF, Gu H (2004) Interface Sci 12:335
17. Huang R, Gu H, Zhang JX, Jiang DL (2005) Acta Mater 53:2521
18. Cliff G, Lorimer GW (1975) J Microsc 103:203
19. Gu H, Cannon RM, Tanaka I, Rühle M (2006) Mater Sci Eng A 422:51
20. Gu H, Tanaka I, Cannon RM, Pan X, Rühle M (2010) Int J Mater Res 101:66
21. Van Rutten JWT, Hintzen HT, Metselaar R (1996) J Eur Ceram Soc 16:995